Escherichia coli detection using thermal images

F. Hahn[1,2]*, G. Hernández[1], E. Echeverría[1] and E. Romanchick[1]

[1]*Departamento de Irrigación, Universidad Autónoma Chapingo, Chapingo, Texcoco, México; and* [2]*VIKSAL, Esmeralda 19, Zihuatanejo, Gro, México. *Email: fhahn@correo.chapingo.mx*

Hahn, F., Hernández, E., Echeverría, E. and Romanchick, E. 2006. ***Escherichia coli* detection using thermal images.** Canadian Biosystems Engineering/Le génie des biosystèmes au Canada **48**: 4.7 - 4.13. Microbiological contamination detection can require a lengthy process. In the present work, a quick and easy methodology was developed to detect *Escherichia coli*, using thermal imaging. *Escherichia. coli* grown on classical LEVINE agar were imaged using a thermal IR camera. A prototype was developed to avoid temperature changes on the surface due to air movement. The prototype which injected heat from the bottom was analyzed thermally to detect relative humidity and temperature changes. The images had to be taken 15 s after taking the Petri dish from the incubator. The thermal images were processed by counting the pixels per color. A RGB processing algorithm worked better than the grey scale algorithm as yellow and rose could not be discriminated properly. The value was introduced in three equations and a detection success rate of 100% was achieved. The minimum time required for detecting microbial contamination was 5 h. **Keywords:** *Escherichia coli* detection, thermal imaging, RGB color processing.

La détection de la contamination microbiologique pourrait avoir besoin de long temps. Dans ce travail une méthodologie rapide et facile a été développée pour détecter L' *Escherichia coli*, en utilisant la formation image thermique. L' *Escherichia coli* crû sur d'agar classique de LEVINE étaient reflètent en utilisant un appareil-photo IR thermique. Un prototype a été développé pour éviter les changements extérieurs de la température due au mouvement d'air. Le prototype qui a injecté la chaleur du fond a été analysé thermiquement afin de détecter ses changements de température et d'humidité. Nous avont constaté que les images ont dû être prises dans le premier 15 secondes après avoir pris les échantillons de l'incubateur. Les images thermiques ont été traitées en comptant le pixel par couleur. Un algorithme traitant RGB a fonctionné mieux que ce qui parant le niveau de gris, étant donné que les couleurs jaune et rose ne pourrait pas être distingué correctement. La valeur a été mise dans trois équations et un taux de 100% était obtenu. Le temps minimum requis pour détecter la contamination microbienne avait lieu dans 5 heures. **Mots clés:** *Escherichia coli* détection, image thermique, RGB algorithme.

INTRODUCTION

Contamination of food and water with *Escherichia coli* can be considered as the last consequence of animal or human fecal shedding. *Escherichia coli* are bacteria commonly found in human and animal intestinal tracts and can survive outside the gastrointestinal tract for considerable time in several environments including soil and water (Ashbolt 2004). *Escherichia coli* have been used as a contamination index of water and food due to the potential dangers that they might cause to human beings. Some *E. coli* strains are food poisoning pathogens that cause from mild to bloody diarrhea and hemolytic uraemic syndrome leading in some cases to permanent disability or death (Stephan et al. 2004). Cultural methods for the isolation and identification of *E. coli* O157, O111, and O26 from contaminated food are time consuming and labour intensive (Catarame et al. 2003), causing difficulties in routine food testing. There is an increasing need in the food industry for rapid and sensitive detection methods.

Microbiological contamination detection is important during food processing and when providing potable water. Microbiological pathogens are normally detected using biochemical and immunologic markers (Chung et al. 2000; Brabetz et al. 1993) or using PCR, polymerase chain reaction (Jothikumar and Griffitths 2002; Fratamico et al. 1995). Molecular detection methods based on PCR are accepted as an alternative to conventional cultural and biochemical methods for the detection of bacterial contamination of food (DeBoer and Beumer 1999). Pathogen prediction has been reported using Raman micro spectroscopy (Osborne 1993), near infrared spectroscopy (Hahn 2004), Fourier transforms photo-acoustic spectroscopy (Irudayaraj et al. 2001) and Fourier transforms infrared spectroscopy (Ellis et al. 2002).

Nevertheless, in most cases large sampling times are required in specialized laboratories. Infrared thermal imaging can determine surface temperature with high precision (Badenas and Caselles 1992; Caselles et al. 1992). Fuller and Wisniewski (1998) reported that the ice nucleation-active bacterium *Pseudomonas syringae* placed on test plants started plant freezing, while Pearce and Fuller (2001) studied barley freezing with infrared video thermography. Kim and Ling (2001) proposed a system based on an infrared detector to measure leaf canopy temperature.

The objective of this work was to detect *Escherichia coli* at their earlier growing stage using a thermal infrared camera. *E. coli* bacterial respiration generates a small but significant amount of heat that can be detected by thermal imaging. A prototype was developed to avoid temperature changes over the sample. To study the behavior, relative humidity and temperature were monitored at the bottom and top of the prototype. Each pixel from the thermal image presented a different temperature color due to the thousands of bacteria contained in it. Two image processing algorithms were tested assuming that after counting the pixels having the same color, bacteria infection could be predicted. A trial group of *Escherichia coli* at different growing stages was used to test three models for predicting biomass production and the models achieved high success rates.

MATERIALS and METHODS

Isolation and identification of *Escherichia coli*

A 1-mL inoculum obtained from urban wastewater was diluted in a 1:10 ratio with a solution containing KH_2PO_4 and $MgSO_4.7H_2O$ at concentrations of 0.425 and 0.25 g/L,

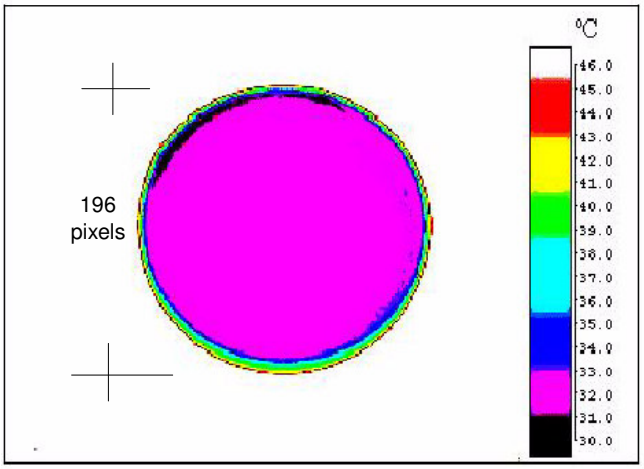

Fig. 1. Infrared measurement obtained in THI format.

respectively. The inoculum was continuously re-diluted in a culture tube until a concentration of 10^{-10} was attained. Each dilution was seeded in a sterile lactose broth (Merck KgaA, Darmstadt, Germany) at a concentration of 13 g/L in five test tubes containing inverted Durham tubes. The tubes were incubated at 35ºC for 24 ± 2 h. When gas was detected in the Durham tubes, microbial growth had occurred; otherwise the culture tubes were incubated for another 24 h.

Microbes inside the last dilution were inoculated with a seedling handle in fermentation tubes containing 10 ± 0.1 mL of the EC broth (*Escherichia coli* broth, Merck KgaA, Darmstadt, Germany). The EC liquid medium was prepared at a concentration of 37 g/L and was incubated for 24 h at 45°C. The isolated culture was applied in grooves over the solid sterile agar (LEVINE emb, Merck KgaA, Darmstadt, Germany) with a concentration of 36 g/L. Inverted Petri dishes were incubated at 35°C for 24 h. This operation was repeated three times to obtain a pure homogeneous culture that showed brilliant red-metallic colonies. Pure cultures of *E coli* in the solid medium were selected to be analyzed with the infrared camera.

Infrared camera and prototype design

An infrared camera (model D500, Raytheon, Inc., Waltham, MA) was used to obtain the thermal images in the 7-14 µm spectral range. A Palm type computer screen inserted in the camera circuit permitted viewing of the focused area. The camera image array was 320 x 240 pixels with its physical circuit size of 15.52 x 11.64 mm. The Petri box was covered with 30,172 pixels (196 pixel diameter) considering each pixel area was 48.5 µm^2 at a focal distance of 400 mm (Fig. 1). The whole image range was 76,800 pixels.

Air movement over a sample during thermal imaging can affect the measurement, so a prototype was developed with two (430 mm long) concentric PVC tubes. The internal diameters of the PVC tubes were 75 and 100 mm and the internal space between them was filled with polyurethane foam to prevent heat loss from the sample surface. A metallic structure fixed the tube to the infrared camera, leaving 400 mm between the camera lens and the Petri dish. A heating plate was installed beneath the Petri dish to maintain the sample temperature within the prototype (Fig. 2).

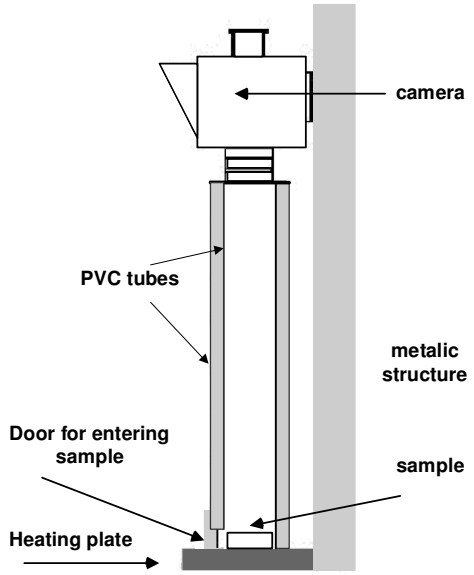

Fig. 2. Prototype for thermal imaging acquisition with heat applied at the sample bottom.

Relative humidity and temperature were monitored with a detector (Humidity meter, Extech Instruments, Waltham, MA) inside the tube at the bottom and at the top of the prototype to study possible condensation on the lens. The thermal behavior within the prototype atmosphere was studied by fixing the initial heating plate temperature at 97ºC. The plate temperature increased to 128ºC after 10 min. A Petri dish prepared with solid sterile agar was introduced at the left bottom side of the prototype after removing the top glass cover. The internal temperature changes within the Petri dish covered with solid sterile agar were monitored with two RTD temperature sensors (LM35DZ, National Instruments, Austin, TX) as shown in Fig. 3a. The temperatures were recorded again on the prototype after inserting the Petri dish onto an expanded polystyrene plate at a height of 10 mm (Fig. 3b).

Sample imaging and image processing

The Petri dish and its mounting place inside the tube were marked to assure its orientation. The infrared measurement was acquired with a prototype atmosphere having a temperature of 37 - 40ºC and relative humidity of 40 – 50%. The Petri dish

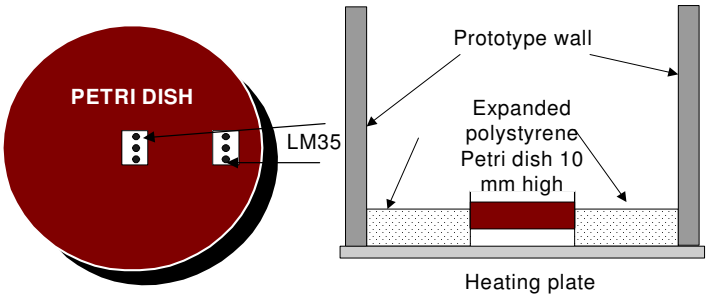

Fig. 3. Petri dish (a) with its sensors inserted; (b) placed at a height of 10 mm above the heating plate and surrounded with expanded polystyrene.

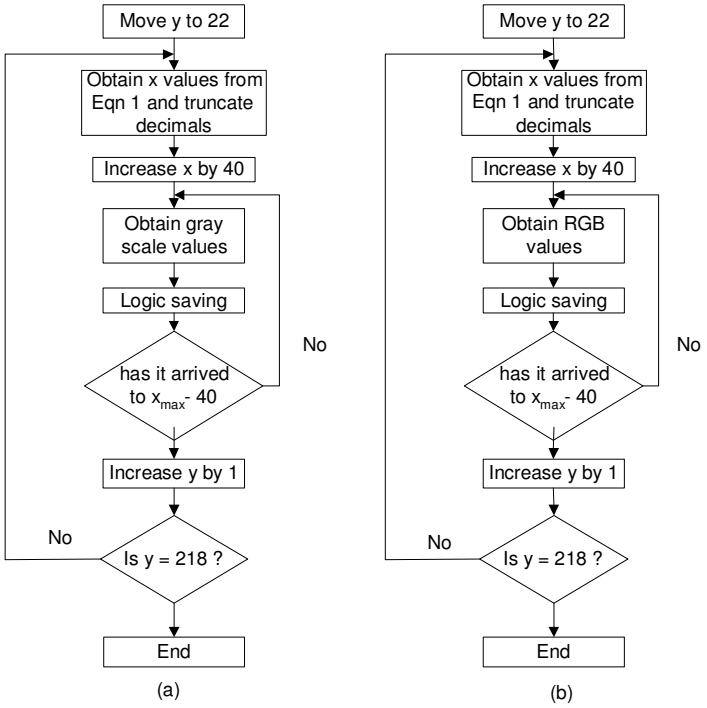

Fig. 4. Algorithms for counting the infected pixels using: (a) grey scale; and (b) RGB colour.

glass cover was removed before the sample was introduced to the prototype. The samples containing *E. coli* were taken from the incubator at 37ºC and images were taken 15 s after being placed in the prototype. It is important to mention that *E. coli* were grown always at 37ºC and their growing pattern is not affected at 40ºC. After applying heat with the plate, the colony's temperature increased to 70ºC after 2 minutes. Images were taken every 15 s and the temperature remained constant.

The acquired images were stored in the infrared camera Compaq iPAQ computer memory using THI format. The Report IR software version 2.0 (Raytheon, Inc., Waltham, MA) opened the THI image files, marked the area of interest, and adjusted the temperature range between 37.32ºC and 37.66ºC, corresponding to black and white, respectively. The color scale is dependent on the temperature ranges used for measurement; so for example, orange is listed as having a temperature of 37.56ºC. The resulting image was stored in BMP format in the main computer (HP Brio, Palo Alto, CA). Two algorithms were developed in C++ for counting those pixels having the same temperature or pixel color. The first image processing algorithm converted the colored image to an eight-bit grey scale and the second-image processing algorithm used RGB bands for classifying each color.

Both algorithms scanned the pixels within the circular Petri dish area centered at coordinates (160,120) as in Eq. 1:

$$(x-160)^2+(y-120)^2=r^2 \quad (1)$$

where:

r = 98 pixels radius, and

x, y = pixel coordinates.

Forty-four rows of the image were unused in the 320 x 240 pixel array as the Petri dish diameter was 196 pixels. The first line scanned by both programs was row number 22. This y coordinate was substituted into Eq. 1 and two different x values were obtained, except for rows 22 (first) and 218 (last), where only one value was obtained. The decimal parts of the X_{min} and X_{max} values were truncated.

Each pixel was scanned and analyzed according to the selected algorithm. The first algorithm (Fig. 4a) converted the color image to an eight bit grey scale image. Each color had an assigned grey scale value, so if it was red (grey scale=101), the red variable acting as a counter was incremented. If it was green the variable green was incremented once. To ignore the measurements taken over the Petri-dish glass wall, the first pixel scanned in each row was (X_{min} + 40, y) and the last was (X_{max} – 40, y). The X_{min} value was incremented until (X_{min} + 40, y) overlapped (X_{max} – 40, y), and when (X_{min} + 40, y) became greater than (X_{max} – 40, y) the following row was scanned until row number 218. The second algorithm (Fig. 4b) got the RGB value of each pixel and the pixel's color was determined based on Table 1. The color variable was used as a counter and incremented every time a pixel had that color. For example, yellow had no blue component, red varied between 248 and 255, and green between 195 and 240 (Table 1). Black RGB values were null, while white presented maximum values.

Table 1. RGB maximum and minimum values for each colour (temperature) and its corresponding grey scale level.

Colour	Temperature (°C)	Grey Level	Red		Green		Blue	
			Min	Max	Min	Max	Min	Max
rose	37.62	224	238	255	180	230	200	254
red	37.58	101	248	255	0	10	0	10
orange	37.56	195	248	255	150	200	0	0
yellow	37.52	225	248	255	195	240	0	0
green	37.48	151	0	5	248	255	0	23
sky blue	37.44	179	0	10	180	248	171	255
dark blue	37.40	30	0	10	0	10	205	255
purple	37.36	89	160	220	0	73	73	198
black	37.32	0	0	0	0	0	0	0
white	37.66	255	255	255	255	255	255	255

Bacteria prediction algorithms

Five thermal images were taken at each growing stage (5, 8, 11, and 22 h after inoculation). The camera focal length was fixed at 400 mm, the emissivity was set at 0.85, and the central temperature was set at 37ºC. A total of 20 samples were inoculated, imaged, and processed and their results were used for obtaining the prediction equations. The average value of each color and

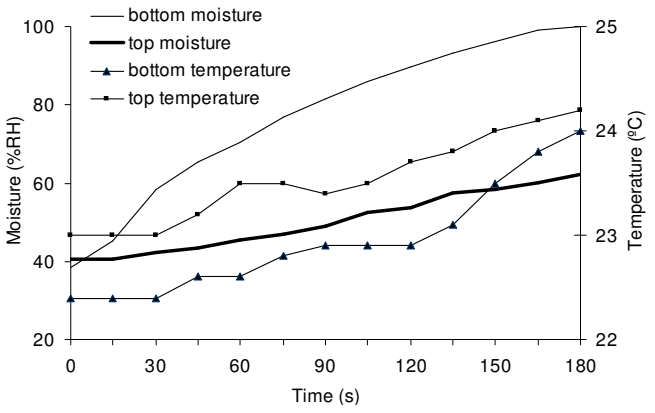

(a)

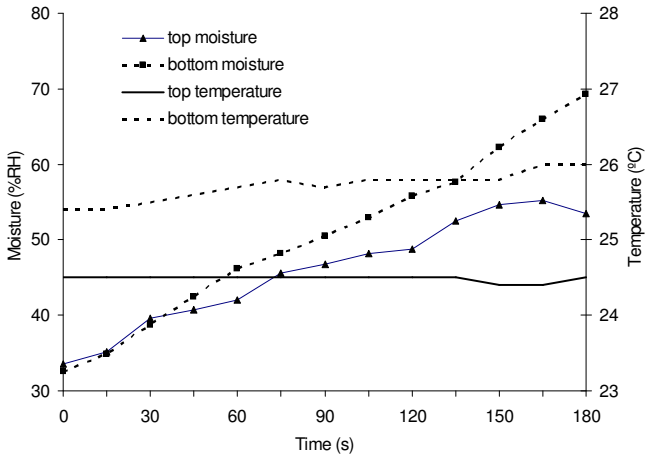

(b)

Fig. 5. Relative humidity and temperature measured at the top and bottom of the prototype: (a) over the heating plate; and (b) inserted on the expanded polystyrene 10 mm above the heating plate.

its standard deviation were obtained. The primary condition to select a color in an equation was to have a high discrimination ratio between non-inoculated samples and inoculated ones. The standard deviation per color was obtained from the counts and used as the second criterion for selecting the best color for *E. coli* detection. The colors applied by the equations presented color-count standard deviations lower than 10. Three equations were proposed to predict bacteria presence (BP) using the average color count values. Detection ranges were proposed for each equation and the detection efficiency was obtained after validating each equation with a trial group of 20 samples (5 for each growing stage).

RESULTS and DISCUSSION

Prototype thermal analysis

The thermal analysis carried out inside the open-topped tube showed that in the bottom of the prototype at 50 mm above the sample the relative humidity increased to 100% after 3 min, with a slope of 0.26%/s (Fig. 5a). At the top, the relative humidity increased to only 60% with a slope of 0.16%/s. When

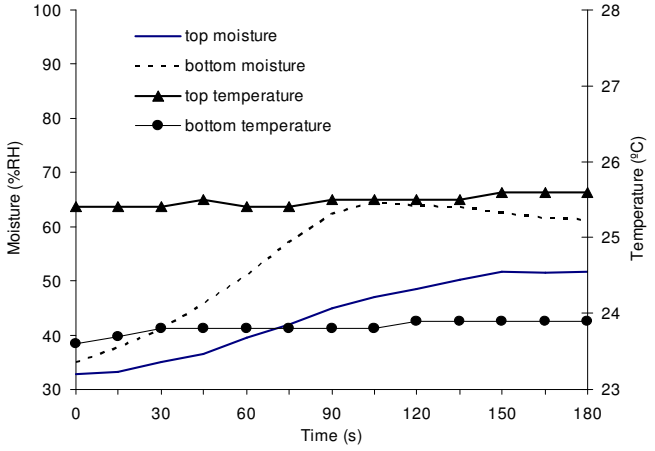

Fig. 6. Relative humidity and temperature of a non-inoculated sterile agar placed inside the prototype without source heating.

the top of the tube was closed, the relative humidity increased 3 times faster. The relative humidity in the top increased to the same value, 60%, that occurred in the bottom after 30 s. The temperature at the top of the prototype was the same as the ambient temperature. Temperature decrease was avoided by placing an expanded polystyrene covering over the heating plate and inserting the Petri dish on polystyrene inside the internal tube.

The temperature inside the bottom of the prototype just over the Petri dish remained constant (± 0.5ºC) although the temperature on the top of the prototype increased 5ºC after 6 min. The relative humidity over the Petri dish increased 35% after 3 min, while at the top it increased 0.092%/s (Fig. 5b) then stayed constant when heated for more time. The prototype worked better with the polystyrene cover as the relative humidity increased 30% less and the temperature did not increment significantly.

As the expanded polystyrene covering had good thermal properties, the heating plate was removed and the temperature and relative humidity changes studied. The relative humidity increased due to gel water evaporation and the temperature was nearly constant during the first 3 min (Fig. 6). No increase was noted during the first 15 s. However, the relative humidity increased to only 50% at the top of the prototype, while it increased to 61% just over the sample. During the next 3 min, the relative humidity was constant inside the prototype.

Two integrated-circuit temperature sensors (LM35) were introduced into the solid agar to study the heat transfer in it. The Petri dish was first placed on the heater plate which was fixed at 97ºC. Measurements were taken every 15 s and the temperatures increased abruptly around the gel after 2.5 min. The samples that had been at ambient temperature (10ºC) increased to 60ºC in the centre and to 80ºC at the border with the dish's glass wall. The gel thickness inside the dish was 8 mm. The glass walls of the Petri dish were hotter and heat was conducted towards the centre of the dish (Fig. 7). When the samples were placed on the polystyrene, the temperature did not increase. The temperature near the dish walls never exceeded 40ºC.

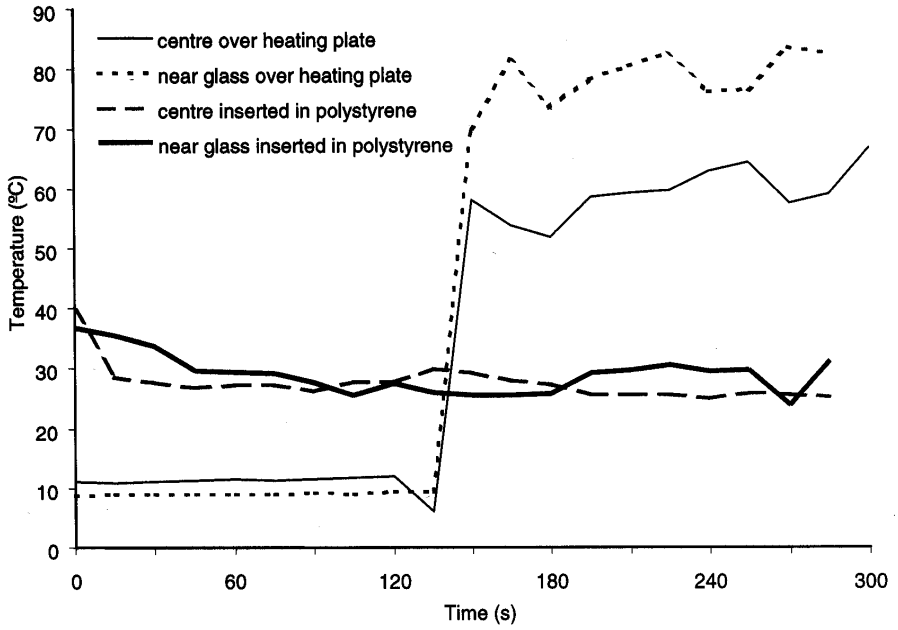

Fig. 7. Temperature measurements inside the Petri dish near the glass wall and at the centre with the sample inserted in polystyrene and over the heating plate.

Escherichia coli detection measurements

Ten different Petri dishes were prepared with solid agar, and five of them were inoculated. Thermal images were acquired 15 s after placing the Petri dish in the prototype and the images were processed to obtain the temperature of each pixel. Thermal differences between samples containing sterile agar and biomass covered agar after 11 h of *E. coli* growth were studied. The numbers of pixels per color were obtained using the RGB algorithm and then averaged. The inoculated samples had higher densities of rose, red, and orange than the control (non-inoculated) samples (Table 2). The difference between each was 0.04ºC. Rose, red, and orange pixels of the infected samples had counts of 714, 1217, and 657, respectively. Blue and purple counts were at least three times greater in the control samples than in the inoculated samples and were eliminated.

Table 3 shows the average count obtained with each algorithm using red, rose, yellow, and orange. Rose and red appeared most. The two image processing algorithms were used to obtain the number of pixels per color. The color counts of the images were averaged and the standard deviation obtained per growing stage. Rose pixels had a standard deviation over ten and were not used in the prediction equations. The increase in red pixels was an index of the quantity of bacteria radiating energy. Yellow and rose grey-scale values were similar, and the program failed in discriminating one from the other. RGB showed a greater difference between those colors with the rose count higher than the yellow one. The yellow counts were constant and independent of bacterial growth stage.

The numbers of red, orange, yellow, and rose pixels were obtained with each program for each image. With the first 20 data (5 per each growing stage) three equations (Eq. 2 to 4) for bacterial presence (BP) were proposed with their applicable intervals.

Table 2. Pixels per colour determined using the RGB algorithm for a control (non-infected) sample and an infected sample after 11 h incubation.

Sample type	Average number of pixels per colour							
	Rose	Red	Orange	Yellow	Green	Sky blue	Dark blue	Purple
Non-infected	0	0	0	228	257	2314	2743	3285
Infected	714	1217	657	514	657	428	143	86

Table 3. Average and standard deviation of each colour count at different growing stages.

Algorithm	Inoculation time (h)	Average count (pixels)				Standard deviation			
		Rose	Red	Orange	Yellow	Rose	Red	Orange	Yellow
Grey	5	78	300	83	72	2.51	2.07	3.78	1.64
Grey	8	98	482	104	104	3.01	2.35	3.52	1.72
Grey	11	121	687	111	125	9.34	4.51	3.58	1.87
Grey	22	510	748	104	485	10.30	5.77	3.27	1.30
RGB	5	138	298	165	62	5.24	2.11	3.22	1.21
RGB	8	293	482	251	64	11.2	2.24	3.11	1.28
RGB	11	455	697	342	64	10.24	3.42	5.82	1.42
RGB	22	1428	842	573	65	14.25	3.11	6.25	1.18

Table 4. Maximum and minimum values predicted by each equation using the grey scale and RGB processing algorithms for counting pixel colour.

Equation number	Counting technique	Predicted values	
		Min	Max
2	Grey	21	63
2	RGB	31	69
3	Grey	7	9
3	RGB	7	9
4	Grey	2.5	3
4	RGB	3	3.5

$$BP = \sqrt[3]{orange^2 + yellow^2} \quad (2)$$

$$BP = \sqrt{\left[\ln(red)\right]^2 + \left[\ln(orange)\right]^2} \quad (3)$$

$$BP = \sqrt[3]{\frac{\left[\ln(red)\right]^2}{h} + \left[\ln(orange)\right]^2} \quad (4)$$

The proposed algorithms used the average values, and the measurements obtained from the entire data ranged from 21 to 63 for Eq. 2. The prediction range was chosen so that 95% of the values obtained from the first 20 images were within the limits. Table 4 shows the minimum and maximum prediction values given by each equation. Table 5 shows the prediction accuracy of *E. coli* detection for each of the three equations tested with a trial group of 20 samples under four growing stages (5, 8, 11, and 22 h). The number of orange and yellow pixels obtained with the grey scale algorithm for each trial image was applied to Eq. 2. The value provided by the equation was positive if the number of pixels was between 30 and 60. The number of positive samples divided by the total provided 75% detection accuracy (Table 5). The same process was carried out for each equation using both image processing algorithms. Although the success rate using grey scale values for Eq. 4 was high (95%), 50% of the calculated BP were 2.96. The system did not provide colony quantification. In the three equations, data failure was encountered in the 5 h samples. Equation 4 was the most accurate but requires knowing the inoculation time, which for research could be an advantage.

CONCLUSIONS

A new method for detecting *E. coli* was tested using an infrared thermal camera. A prototype was developed to avoid temperature changes in the sample and moisture condensation on the lens. Prediction of bacteria colonies can be achieved in less time than with traditional techniques. In future work, *E. coli* should be applied to vegetable and meat surfaces to determine whether they can be detected quickly.

Temperature and relative humidity changes in the prototype can be avoided if the images are acquired within 15 s of inserting the sample. The relative humidity increased rapidly when a Petri dish was inserted into the prototype. The plate temperature had to be controlled because the temperature inside the Petri dish, when using the heating plate, varied between the wall and the centre. However, the prototype worked without a heating plate because expanded-polystyrene under the sample maintained the temperature constant for more than 15 s.

Table 5. *Escherichia coli* detection success rates for the three equations within the given interval ranges.

Equation number	Interval	Detection accuracy (%)	
		Grey	Colour
2	30<BP<60	75	80
3	7<BP<9	80	90
4	2.5<BP<3.5	95	100

The RGB algorithm was more efficient than the grey scale algorithm. Rose and yellow grey-scale values presented a difference of 1 and were difficult to discriminate. Blue and purple counts were three times higher in non inoculated samples than in inoculated samples and were not used in the prediction algorithms. Three models using yellow, orange, and red counts successfully predicted *E. coli.* A prediction accuracy of 100% was obtained with Eq. 4 and had the advantage that the inoculation time was included. Equation 3 provided 90% prediction accuracy but did not include inoculation time.

ACKNOWLEDGMENTS

We thank Dr. William E. Muir from the Department of Biosystems Engineering, University of Manitoba, who kindly assisted us in editing the paper and gave us valuable suggestions during the development of this paper.

REFERENCES

Ashbolt, N.J. 2004. Microbial contamination of drinking water and disease outcomes in developing regions. *Toxicology* 198: 229-238.

Badenas, C. and V. Caselles. 1992. A simple technique for estimating surface temperature by means of a thermal infrared radiometer. *International Journal of Remote Sensing* 13: 2951-2956.

Brabetz, W., W. Liebl and K.H. Schleifer. 1993. Lactose permease of Escherichia coli catalyzes active beta-galactoside transport in a gram-positive bacterium. *Journal of Bacteriology* 175(22): 7488-7491.

Caselles, V., J.A. Sobrino and C. Coll. 1992. On the use of satellite thermal data for determining evapotranspiration in partially vegetated areas. *International Journal of Remote Sensing* 13: 2669-2682.

Catarame, T.M.G., K.A. O'hanlon, G. Duffy, J.J. Sheridan, I.S. Blair and D.A. McDowell. 2003. Optimization of enrichment and plating procedures for the recovery of Escherichia Coli O111 and O026 from minced beef. *Journal of Applied Microbiology* 95: 949-957.

Chung, K.S., C.N. Kim and K. Namgoong. 2000. Evaluation of the Petrifilm rapid coliform count plate method for coliform enumeration from surimi-based imitation crab slurry. *Journal of Food Protection* 63(1):123-125.

DeBoer, E. and R.R. Beumer. 1999. Methodology for detection and typing of food borne microorganisms. *International Journal of Food Microbiology* 50: 119-130.

Ellis, D., D. Broadhurst, D.B. Kell, J. Rowland and R. Goodacre. 2002. Rapid and quantitative detection of the microbial spoilage of meat by Fourier transform infrared spectroscopy and machine learning. *Applied and Environmental Microbiology* 68: 2822-2828.

Fratamico, P.M, S.K. Sackitey, M. Wiedmann and M.Y. Deng. 1995. Detection of Escherichia coli O157:H7 by multiplex PCR. *Journal of Clinical Microbiology* 33(8): 2188-2191.

Fuller M.P. and M. Wisniewski. 1998 The use of infrared thermal imaging in the study of ice nucleation and freezing of plants. *Journal of Thermal Biology* 23: 81-89.

Hahn F. 2004. Spectral detection and neural networks discrimination of *Rhizopus Stolonifer* spores in red tomatoes. *Biosystems Engineering* 89(1):93-99.

Kim, Y. and P. P. Ling. 2001. Machine visions guided sensor positioning system for leaf temperature assessment. *Transaction of the ASAE* 44(6): 1941-1947.

Irudayaraj, J., H. Yang and S. Sivakesava. 2001. Detection of microorganisms on food surface using Fourier transform photoacoustic spectroscopy. *Journal of Molecular Structure* 606:181-188.

Jothikumar, N. and M. W. Griffitths. 2002. Rapid detection of Escherichia coli 0157:H7 with Multiplex Real-Time PCR Assays. *Applied and Environmental Microbiology* 68: 3169-3171.

Osborne, B.G. 1993. *Near Infrared Spectroscopy in Analysis*, 2nd edition. Singagpore: Longman Singapore Publishers Limited.

Pearce, R S. and M.P. Fuller. 2001. Freezing of barley studied by infrared video termography. *Plant Physiology* 125:227-240.

Stephan R, N. Borel, C. Zweifel, M. Blanco and J.E. Blanco. 2004. First isolation and further characterization of enteropathogenic Escherichia coli (EPEC) O157:H45 strains from cattle. *BMC Microbiology* 4: 10.